Device

Article

In vivo monitoring of tissue permeability in a rat colitis model via a bioimpedance-sensing ingestible device

Graphical abstract

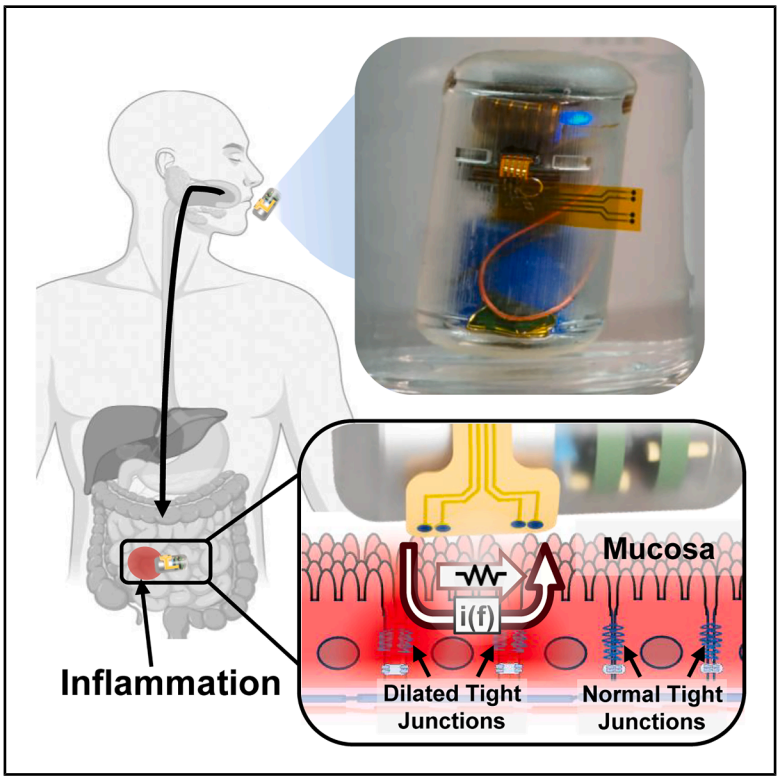

Authors

Mateo W. Lim, Hammed Ayansola, Justin M. Stine, Julie M. Karasik, Younggeon Jin, Reza Ghodssi

Correspondence

ghodssi@umd.edu

In brief

Bioimpedance sensing is a promising method for monitoring mucosal permeability, a subclinical sign of gastrointestinal (GI) inflammation. We present the fabrication and evaluation of a bioimpedance-sensing ingestible capsule for minimally invasive monitoring of inflammatory bowel disease (IBD). PEDOT:PSS electrodes demonstrate stability in simulated GI conditions. The device is evaluated *ex vivo* on excised mouse colon tissue and *in vivo* implanted in a DSS-induced rodent colitis model.

Highlights

- Bioimpedance sensing enables real-time measurement of mucosal permeability
- PEDOT:PSS electrodes demonstrate stability in simulated GI conditions
- Integrated system supports low-power sensing and wireless communication
- Capsule measures alterations in inflamed tissues in a rodent colitis model

Develop
Prototype with demonstrated applications in relevant environment

Lim et al., 2026, Device *4*, 101180
July 17, 2026
https://doi.org/10.1016/j.device.2026.101180

CellPress

Please cite this article in press as: Lim et al., *In vivo* monitoring of tissue permeability in a rat colitis model via a bioimpedance-sensing ingestible device, Device (2026), https://doi.org/10.1016/j.device.2026.101180

Device

CellPress

Article

In vivo monitoring of tissue permeability in a rat colitis model via a bioimpedance-sensing ingestible device

Mateo W. Lim,[1,2,3] Hammed Ayansola,[4] Justin M. Stine,[5] Julie M. Karasik,[6] Younggeon Jin,[4] and Reza Ghodssi[1,2,3,5,7,*]
[1]Department of Electrical and Computer Engineering, University of Maryland, College Park, MD 20742, USA
[2]Institute for Systems Research, University of Maryland, College Park, MD 20742, USA
[3]Robert E. Fischell Institute for Biomedical Devices, University of Maryland, College Park, MD 20742, USA
[4]Department of Animal & Avian Sciences, University of Maryland, College Park, MD 20742, USA
[5]MATRIX Lab, University of Maryland, College Park, MD 20742, USA
[6]Fischell Department of Bioengineering, University of Maryland, College Park, MD 20742, USA
[7]Lead contact
*Correspondence: ghodssi@umd.edu
https://doi.org/10.1016/j.device.2026.101180

THE BIGGER PICTURE Inflammatory bowel diseases (IBDs), such as Crohn's disease and ulcerative colitis, are among the most prevalent gastrointestinal (GI) disorders. Traditional endoscopy is the gold standard for IBD diagnostics through visualization, but this method is highly invasive and often only effective once symptoms are exacerbated. Mucosal permeability is a subclinical biomarker indicative of the assessed GI inflammation.

SUMMARY

Inflammation in the gastrointestinal (GI) tract is closely associated with increased mucosal permeability. Quantifying mucosal permeability in GI tissue can help monitor and localize inflammation caused by inflammatory bowel disease (IBD). Bioimpedance sensing can noninvasively measure region-specific impedance, quantifying its permeability. This work presents a bioimpedance-sensing capsule capable of wirelessly monitoring mucosal permeability for monitoring IBD. Electropolymerized poly(3,4-ethylenedioxythiophene) polystyrene sulfonate (PEDOT:PSS) electrodes decrease interfacial impedance, improving charge storage capacity (CSC) 375-fold relative to metal electrodes. Capsule package integrity and sensor performance are evaluated in physiologically relevant GI fluids, confirming long-term operation suitable for GI transit with low sensor variability. Bioimpedance measurements via the ingestible device on ethylenediaminetetraacetic acid (EDTA)-treated mouse colon tissue quantify mucosal permeability changes from junctional disruptions. The ingestible device is implanted and tested in a rodent colitis model, demonstrating the ability to detect alterations in mucosal permeability of inflamed tissue *in vivo* at different stages of IBD progression.

INTRODUCTION

Inflammatory bowel disease (IBD) causes chronic inflammation throughout the gastrointestinal (GI) tract and is linked to compromised epithelial barrier integrity, altered gut microbiota composition, and systemic immune dysregulation. Despite advances in treatment, the global burden of IBD remains high, with prevalence continuing to rise steadily in Western countries and incidence increasing rapidly in newly industrialized countries. Forecasts predict that 1% of the population will be afflicted with IBD by 2030.[1] Under normal physiological conditions, the intestinal epithelium forms a selectively permeable barrier that allows movement of essential nutrients and ions while preventing the passage of harmful microbes and their products.[2] In pathological conditions, increased mucosal permeability allows bacteria and their products to penetrate the mucosa, promoting immune activation and inflammation while altering tissue dielectric properties. Relative changes in mucosal conductivity reflect alterations in tight junction (TJ) barrier dilation, cellular membrane integrity, and extracellular ion content, which can indicate localized mucosal damage.[3]

Current IBD diagnosis primarily relies on a review of patient symptom history, physical examination, and blood and fecal biomarkers (e.g., C-reactive protein and fecal elastase). Endoscopic procedures and capsule endoscopy devices, such as the PillCam,[4] are employed to visualize the GI tract and often require

Please cite this article in press as: Lim et al., *In vivo* monitoring of tissue permeability in a rat colitis model via a bioimpedance-sensing ingestible device, Device (2026), https://doi.org/10.1016/j.device.2026.101180

subsequent tissue biopsy for definitive diagnosis.[5] While visualization methods are the gold standard for IBD diagnosis, they are not ideal for continuously monitoring epithelial barrier dysfunction because microscopic damage can occur with minimal visible response, yet detecting these subtle changes is critical for evaluating early subclinical inflammation and mucosal healing. Other diagnostic methods, such as fecal and serum sampling, provide a noninvasive alternative to traditional endoscopy[6]; however, these methods are nonspecific and often only effective when severe symptoms are already present. Together, these limitations underscore the need for minimally invasive methods capable of continuously assessing intestinal mucosal integrity to better understand IBD pathogenesis and guide the development of effective therapeutic interventions.

Impedimetric techniques have emerged for measuring the electrical properties of GI tissues associated with mucosal permeability, overcoming conventional diagnostic limitations. Transepithelial electrical resistance (TEER) measurements, considered the gold standard for assessing barrier integrity, quantify the electrical resistance across a cellular monolayer.[7] Typically, with TEER, biopsied tissue is mounted in a Ussing chamber, where electrodes positioned on either side of the sample measure transepithelial resistance.[8] However, a major drawback of this method is that it is unable to measure mucosal integrity *in vivo* and requires invasive biopsy. Similarly, electric cell-substrate impedance sensing (ECIS) measures the electrical impedance of a cell layer grown on planar, circular gold (Au) electrodes.[9] ECIS measurements occur over a range of frequencies, allowing characterization of intra- and extracellular space from capacitive contributions.[9] While TEER and ECIS can quantify mucosal permeability of tissue and epithelial cells, they have only been implemented in a research setting and cannot provide useful clinical data without frequent invasive sampling of the GI tract. Alternatively, molecular probes, such as lactulose-mannitol and sucrose,[10,11] are ingested and examined from excreted urine to noninvasively monitor intestinal permeability; however, they cannot specify the location of barrier dysfunction.

Ingestible devices provide a noninvasive platform for real-time assessment of the entire GI tract.[12] In addition to endoscopic capsules (e.g., PillCam) for visualizing the GI tract, ingestible devices have been developed that are capable of sensing biomarkers such as pH,[13] temperature,[14] gas,[15] oxidation-reduction potential (ORP),[16] and tissue luminance.[17] While current sensing ingestible devices provide information about a patient's gut health, few have modalities that can monitor epithelial barrier function. There have been recent developments in capsule systems for IBD diagnosis that rely on magnetic actuation for biopsy and tissue elasticity sensing.[18,19] While these works have promising capabilities of assisting with IBD diagnostics, they require external magnetic systems, making profiling of the GI tract discontinuous and more complex. This leaves a gap in technologies capable of continuously and noninvasively monitoring epithelial permeability and localizing sites of inflammation *in situ*. Integrating bioimpedance sensing, which directly measures tissue dielectric properties,[20] into an ingestible capsule addresses the unmet challenge for longitudinal monitoring of GI epithelial integrity. Bioimpedance sensors feature coplanar electrodes that directly contact the tissue; during measurements, alternating current is applied, and the voltage response is measured, yielding impedance magnitude and phase data over a range of frequencies.[21] Flexible bioimpedance sensors have already been implemented commercially in wearable devices for monitoring of dermal biological materials,[22] but adaptation for use within the GI tract remains largely unexplored. Ingestible devices have demonstrated the ability to monitor epithelial permeability in inflammatory conditions such as eosinophilic esophagitis (EoE) and gastroesophageal reflux disease (GERD) via impedance sensing.[23,24] However, packaging and communication challenges have limited their operation from regions beyond the esophagus, making them unable to access the small and large intestine, where inflammation related to IBD manifests.

Several challenges arise when adapting tissue-interfacing technology for GI transit. Microelectrodes are often used for *in situ* measurement of impedimetric biomarkers through electrochemical impedance spectroscopy (EIS).[25] However, interface impedances must be mitigated to avoid low signal-to-noise ratios (SNRs) and reduced sensor performance.[26] Often, conductive surface modification materials such as platinum (Pt) black,[27] carbon nanotubes (CNTs),[28] iridium oxide (IrOx),[29] and polymeric films (e.g., poly(3,4-ethylenedioxythiophene) polystyrene sulfonate [PEDOT:PSS], polypyrrole [PPy], and polythiophene [Pth])[30–32] are utilized to decrease interface impedance and increase the charge storage capacity (CSC) of the sensing electrode. Biocompatible materials must be selected to prevent adverse biological response from ingestion of the device. High pH variability and various enzymes, acids, and bacteria throughout the GI tract can cause sensor and package degradation,[33] making device operation ineffective. Additionally, the length and limited diameter of different regions, as well as peristaltic forces acting on the device, can disrupt orientation[34] and affect measurement reliability. These challenges necessitate small electronic components packaged in a compact form factor capable of withstanding the GI environment and maintaining reliable sensing capability. Holt et al.[35] reported an ingestible bioimpedance-sensing device for wireless sensing of tissue impedance. This device was validated using *ex vivo* mouse colonic tissue treated with a calcium chelator (ethylenediaminetetraacetic acid [EDTA]) to induce TJ dilation, showing reduced impedance magnitude, which corresponds with the relative measurement of transepithelial resistance in a Ussing chamber.[35] However, challenges related to packaging and sensor stability impeded *in vivo* testing, highlighting the need for packaging improvements and sensor optimization of the wireless bioimpedance device.

This work presents an ingestible capsule capable of bioimpedance sensing directly on GI tissues to monitor mucosal permeability (Figure 1A). The system comprises tetrapolar electrodes electropolymerized with PEDOT:PSS to improve sensor performance and electrode-film adhesion over previous electrodeposition methods.[35] The integrity of the PEDOT:PSS sensor and capsule package prevented significant sensor drift and capsule leakage when submerged in physiologically relevant simulated GI fluids. The functionality of the assembled device to detect altered mucosal permeability was characterized in excised colonic mouse tissues with varying degrees of TJ dilation induced by calcium chelation (Figure 1B). The bioimpedance

Please cite this article in press as: Lim et al., *In vivo* monitoring of tissue permeability in a rat colitis model via a bioimpedance-sensing ingestible device, Device (2026), https://doi.org/10.1016/j.device.2026.101180

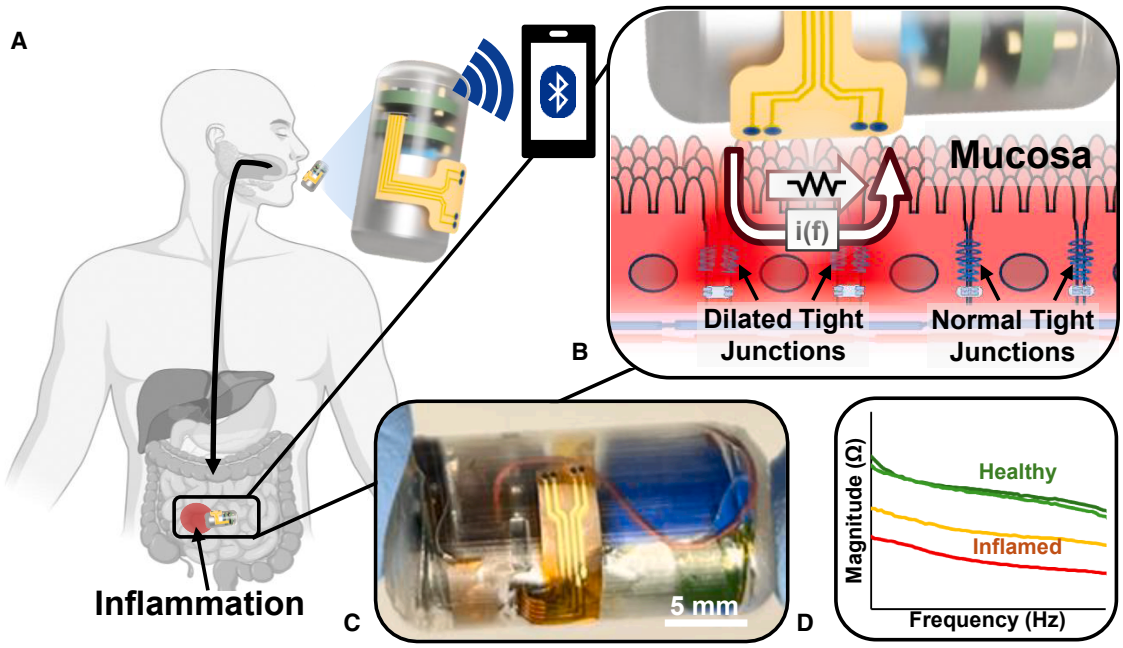

Figure 1. Depiction of capsule operation and principle

(A) Schematic overview of the bioimpedance-sensing capsule localizing inflammation in the gastrointestinal tract and wirelessly reporting data.

(B) Conceptual illustration of bioimpedance sensor measuring mucosal permeability through TJ dilation.

(C) Microscope image of integrated ingestible device with bioimpedance sensor.

(D) Representative impedance spectra of healthy vs. inflamed tissue.

ingestible device (Figure 1C) distinguishes healthy from inflamed tissue *in vivo* in control and colitis rodent models (Figure 1D), demonstrating the detection of barrier dysfunction. This work marks a significant advancement toward noninvasive monitoring of mucosal permeability for the detection and localization of inflammation throughout the GI tract.

RESULTS AND DISCUSSION

PEDOT:PSS bioimpedance sensor design and fabrication

The bioimpedance sensor consists of four electrodes arranged in a Wenner/Schlumberger configuration, where current is injected through the outer electrodes and the resulting voltage difference of the medium is measured across the inner electrodes, significantly reducing contact impedance.[36] This arrangement creates a region highly sensitive to changes in impedance between the sensing electrodes, where electrode spacing and dimensions control the depth of the sensitivity region.[21] Previous work optimizes electrode spacing and dimensions using a finite-element model to simulate electric field lines through intestinal tissue; these simulations demonstrate an inner electrode spacing of $\leq$1.6 mm for high sensitivity and field confinement to mucosal and submucosal tissue layers under healthy and inflamed conditions.[35] Gold (Au) electrodes (inner electrode spacing: 1 mm, Ø = 0.5 mm) are patterned onto a flexible polyimide substrate using photolithography and a standard lift-off process (Figure 2A), allowing the sensor to easily conform to the outside of the ingestible device. To insulate the conductive traces, the sensor was coated with a biocompatible Parylene-C layer, and the electrode and contact pad areas were selectively exposed by reactive ion etching (RIE) (Figure 2B).[35] Following fabrication, individual sensors were cut out of the polyimide substrate, and a polyvinyl chloride (PVC) adhesive backing was applied to the contact pads to facilitate connection between the sensor and electronics (Figure 2C).

While Au is commonly used as an electrode material due to its biocompatibility and chemical inertness,[37] Au electrodes tend to have high interfacial impedance resulting from double-layer capacitive effects at the electrode-electrolyte interface.[38] To reduce interfacial impedance, sensor electrodes were modified with a conductive PEDOT:PSS film, improving the SNR. PEDOT:PSS was chosen for its high conductivity, biocompatibility, and limited fouling, making it a common electrode material for planar neural electrodes.[39] Common PEDOT:PSS fabrication techniques include spin coating,[40] electrodeposition,[35] and electropolymerization.[30] Here, electropolymerization was chosen over other deposition methods due to its uniform surface coverage and superior film adhesion.[30] The PEDOT:PSS film was electropolymerized onto the sensing electrodes using a benchtop potentiostat (BioLogic VSP300) in an aqueous solution of 10 mM EDOT and 2% w/v PSS (Figure 2D). The solution composition satisfied the critical micellar concentration of PSS, allowing for a homogeneous dispersion of EDOT.[41] A constant current density of 5 $\mu A/mm^2$, as optimized by Starbird et al.,[41] was applied via chronopotentiometry (CP) for 180 s to polymerize EDOT directly onto the Au electrodes, forming a uniform PEDOT:PSS film. The resulting chronopotentiogram exhibited a

Please cite this article in press as: Lim et al., *In vivo* monitoring of tissue permeability in a rat colitis model via a bioimpedance-sensing ingestible device, Device (2026), https://doi.org/10.1016/j.device.2026.101180

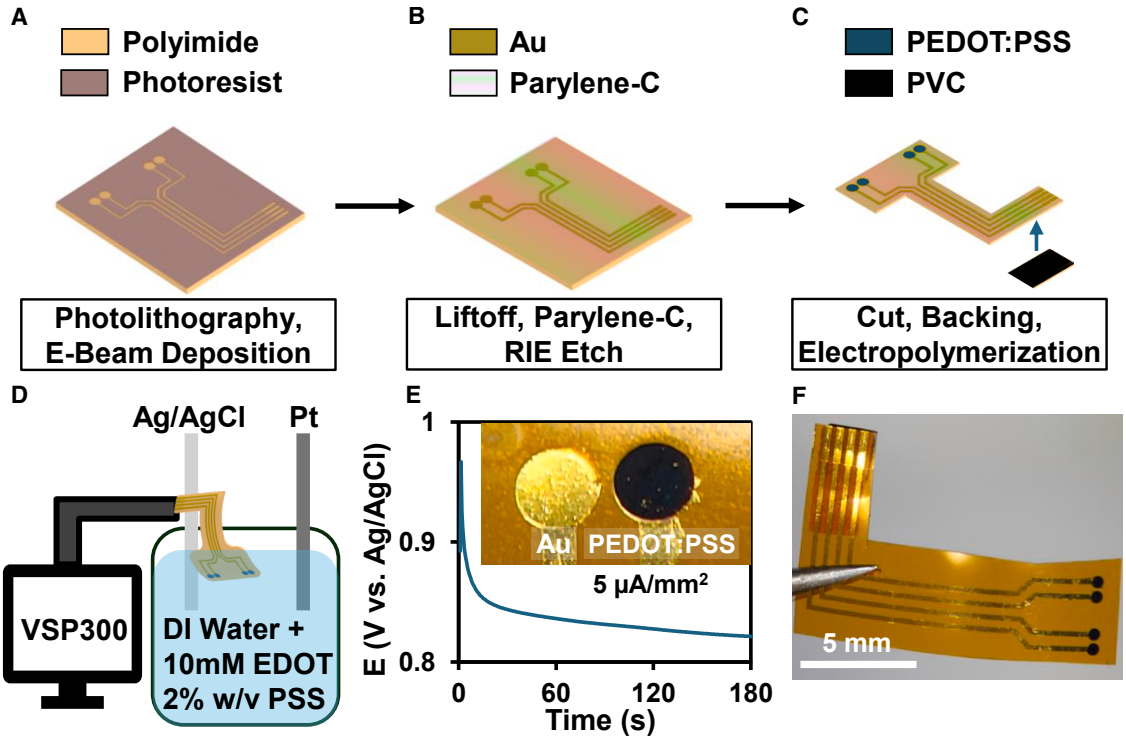

Figure 2. Bioimpedance sensor fabrication

(A) Au is patterned on polyimide substrate using electron-beam evaporation and a standard lift-off process.

(B) Parylene-C is coated over the wafer for insulation, and electrodes and contact pads are exposed through RIE.

(C) Individual sensors are cut out, and a PVC adhesive stiffener is applied to the backside of the contact pads. Electrodes are electropolymerized with PEDOT:PSS.

(D) PEDOT:PSS electropolymerization (EP) protocol with a Pt counter electrode and silver/silver chloride (Ag/AgCl) reference electrode.

(E) Chronopotentiogram of EP confirming PEDOT:PSS deposition; Au electrodes before and after EP (inset).

(F) Microscope image of fabricated sensor.

characteristic increase in voltage followed by an exponential plateau, confirming successful film formation (Figure 2E). This protocol enables high-throughput fabrication of Au electrodes modified with PEDOT:PSS on flexible substrates for bioimpedance sensing (Figure 2F).

Sensor characterization in simulated fluids

To assess the quality of the PEDOT:PSS film, the CSC of bare Au and PEDOT:PSS electrodes was characterized by cyclic voltammetry (CV) in a phosphate-buffered saline (PBS) solution using the same potentiostat electrode setup. Voltage sweeps from −0.5 to +0.5 V (100 mV/s scan rate) resulted in a 375 ± 2.2-fold increase in CSC for the PEDOT:PSS sensor electrodes compared to bare Au (Figure 3A). EIS curves of bare Au and PEDOT:PSS sensors are compared at physiologically relevant ionic concentrations (∼150 mM)[42] using an integrated circuit (IC) potentiostat evaluation board (EVAL-AD5940BIOZ). Impedance magnitude and phase data were recorded over a 100 Hz–200 kHz frequency sweep for $N = 3$ sensors. The PEDOT:PSS sensor exhibited a stable, frequency-invariant, impedance response (±1.5 Ω, ±0.13°) (Figures 3B and 3C). Bare Au electrodes exhibited high-magnitude impedance and varying phases, especially at lower frequencies. The higher impedance and phase dependence align with expected double-layer capacitances, which are particularly present at these lower frequencies from the Au electrodes. The stability of the PEDOT:PSS electrodes demonstrates the capability of the conductive polymer film to significantly reduce interfacial impedance. To assess the ion sensitivity of the bioimpedance sensor, EIS measurements were taken at physiologically relevant concentrations found in the small intestine. The PEDOT:PSS sensor exhibited a linear response of −0.51 Ω/mM at a fixed frequency (10 kHz, ±0.13 Ω) as the NaCl concentration was increased from 150 to 200 mM, representing sufficient sensitivity to differentiate small changes in ionic concentration found in the intestines (Figure S1).[42]

Long-term *in vivo* operation of sensors requires addressing sensor degradation related to the harsh GI environment. To quantify sensor drift, measurements were taken in simulated gastric fluid (SGF; pH 1.0–1.4, Ricca Chemicals) and simulated intestinal fluid (SIF; pH 6.7–6.9, Ricca Chemicals). EIS measurements from 100 Hz to 100 kHz were recorded at 5-min intervals over two 90-min periods at 37°C with the EVAL-AD5940BIOZ development kit (Analog Devices, Wilmington, MA, USA) while

Please cite this article in press as: Lim et al., *In vivo* monitoring of tissue permeability in a rat colitis model via a bioimpedance-sensing ingestible device, Device (2026), https://doi.org/10.1016/j.device.2026.101180

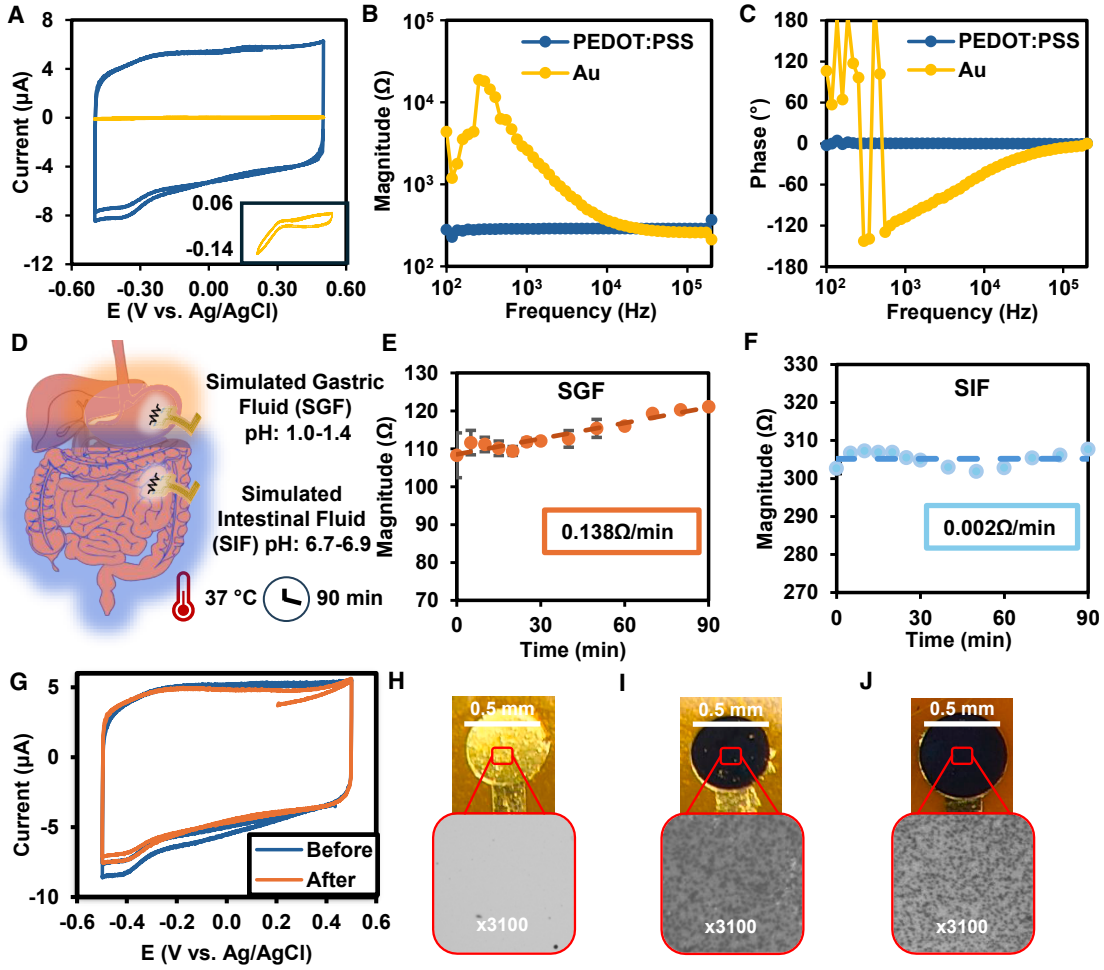

Figure 3. Bioimpedance sensor characterization

(A) Cyclic voltammogram comparing Au and PEDOT:PSS sensors in 1× PBS.
(B) Bode plot of magnitude impedance over 100 Hz–200 kHz comparing Au and PEDOT:PSS sensors.
(C) Phase of Au and PEDOT:PSS sensors.
(D) Overview of testing in simulated GI fluid.
(E) Average impedance of sensor over 90 min in SGF.
(F) Average impedance of sensor over 90 min in SIF.
(G) Cyclic voltammogram comparing the electrode before and after SGF exposure.
(H) SEM image of bare Au electrode.
(I) SEM image of uniform PEDOT:PSS coverage.
(J) SEM image of PEDOT:PSS coverage after 90 min in SGF.
Error bars shown as standard deviation (SD) of mean.

the sensor was first immersed in SGF, then immediately transferred to SIF to simulate the effects of transiting from the stomach to the intestines. Overall, the impedance measurement remained invariant with frequency; hence, 10 kHz was selected for analysis due to its previously demonstrated stability for quantifying intestinal tissue permeability *ex vivo*.[35] Initially, the capsule was exposed to low-pH SGF for 90 min. EIS results showed a small 0.138 Ω/min drift (Figure 3D), equating to only a ∼5% shift in base impedance for typical fasted gastric emptying times with endoscopic capsules (∼30 min).[43] After exposure to SGF, the sensor was immediately translated to SIF. EIS measurements exhibited a negligible drift (0.02 Ω/min) over 90 min (Figure 3F), demonstrating that SGF exposure did not affect the sensor's subsequent performance in SIF and supporting that PEDOT:PSS sensors are resilient against drift in simulated GI environments. Additional CV measurements and scanning electron microscopy (SEM) images were taken before and after exposure to the low-pH SGF to assess its effects on the PEDOT:PSS film and sensor performance. CVs before and after 2.5-h SGF exposure at 37°C show a small 7% decrease in CSC for PEDOT:PSS sensors. SEM images (3,100×-magnification) of the sensor confirm the integrity of the PEDOT:PSS surface morphology after exposure to SGF (Figures 3H–3J). Evaluation of the PEDOT:PSS sensor in simulated GI fluids demonstrated

Please cite this article in press as: Lim et al., *In vivo* monitoring of tissue permeability in a rat colitis model via a bioimpedance-sensing ingestible device, Device (2026), https://doi.org/10.1016/j.device.2026.101180

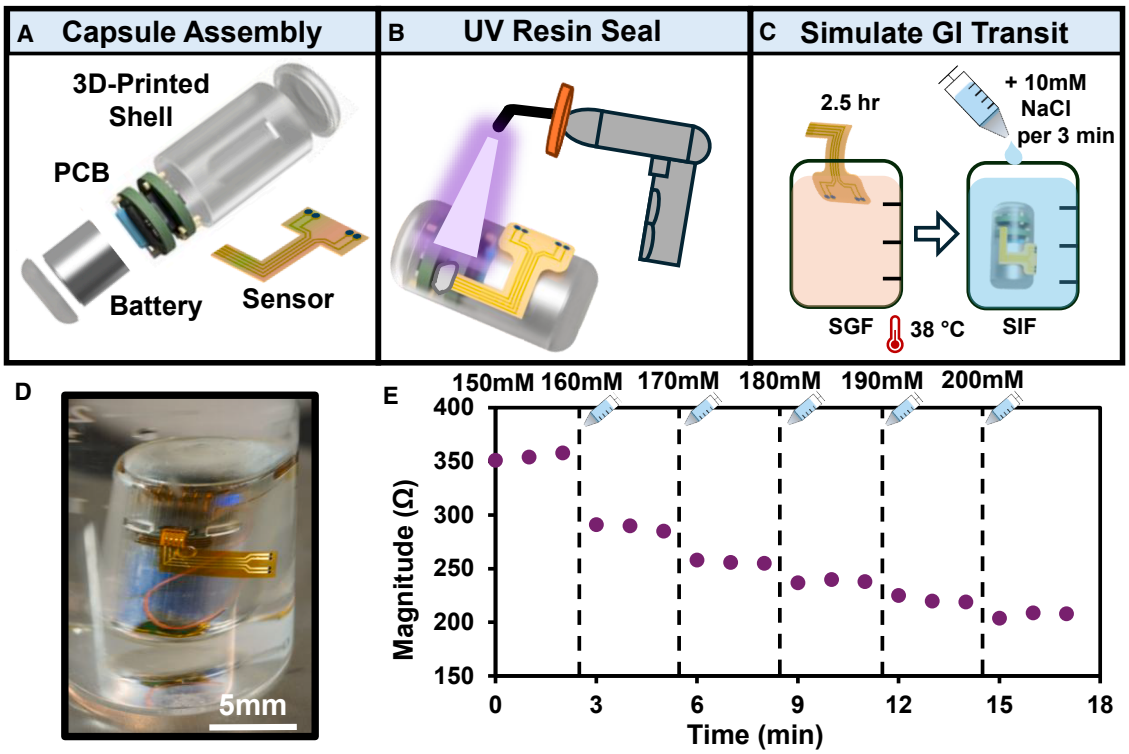

Figure 4. Capsule assembly and validation in simulated fluids

(A) A computer-aided design (CAD) rendering of a bioimpedance capsule device with internal electronics and battery encapsulated in a 3D-printed resin capsule shell packaging with an external bioimpedance sensor connected through a sealable port on the packaging.

(B) The assembled capsule is sealed with biocompatible UV resin.

(C) Experimental protocol of device testing in simulated GI fluids.

(D) Ingestible device submerged in SIF during BLE communication.

(E) Real-time magnitude impedance measured via an ingestible device as ionic strength is increased.

Error bars shown as standard deviation (SD) of mean.

physical and electrochemical resilience to dynamic GI conditions, supporting the PEDOT:PSS sensor's suitability for *in vivo* GI operation.

Ingestible sensor capsule design and assembly

To locally measure bioimpedance, PEDOT:PSS sensors were integrated into a wireless ingestible capsule together with custom printed circuit board (PCB) electronics capable of real-time EIS measurements and Bluetooth Low Energy (BLE) wireless communication and powered by a lithium-manganese dioxide ($LiMnO_2$) battery. Preventing contamination and ensuring isolation of the internal component while still enabling interconnection with external sensors is paramount for safety and functionality during *in vivo* studies. To ensure compliance with the US Food and Drug Administration (FDA) guidance on packaging medical devices,[44] biocompatible 3D-printable resins are often used to encapsulate capsule electronics, creating a durable package that can withstand the GI environment.[45] However, even with robust materials, effective sealing is needed to prevent leakage of biofluids to the electronics and battery and internal components, especially when sensors or actuators are interfaced with the GI environment. A biocompatible capsule shell was fabricated from surgical guide resin (Formlabs, Somerville, MA, USA) using LCD 3D printing to package the custom PCB electronics and battery (Figure 4A), isolating these components from the GI environment. The capsule shell packaging (14 × 28 mm) features a port to interface the sensor via a flat-flex connector (FFC) to connect internal electronics to the GI-interfacing bioimpedance sensor and internal alignments for PCBs to facilitate connection with the FFC through the capsule port (Figure S2). Two rounded "cap" pieces fit into the ends of the capsule shell. To seal the capsule packaging, surgical guide resin was injected into the sensor port and in the seams between the main shell body and caps; subsequent ultraviolet (UV) curing of the resin created a watertight and stable seal (Figure 4B). The capsule packaging scheme successfully isolates internal electronics and batteries from the GI environment while enabling the bioimpedance sensor to interface with GI tissue. Current dimensions exceed commercially available capsule systems, raising concerns about obstruction and altered motility. Future work will focus on conforming to the US FDA standard capsule size "000" (10 × 26 mm) before large-animal testing.

To assess the integrity of the capsule packaging and sealing, empty capsule shells with an external sensor assembled were filled with blue dye. Sealed packages were placed in SGF and SIF for 2.5 and 8 h, respectively, at 37°C under sonication to

Please cite this article in press as: Lim et al., *In vivo* monitoring of tissue permeability in a rat colitis model via a bioimpedance-sensing ingestible device, Device (2026), https://doi.org/10.1016/j.device.2026.101180

emulate peristaltic and environmental conditions during capsule transit in the GI tract.[34] Capsule shells (N = 4) did not exhibit leakage of the blue dye. This assessment in simulated GI fluids demonstrated sealing methods for a durable, watertight package suitable for GI transit (Figure S3).

After the sealing integrity was confirmed through simulated fluid evaluation, all components were assembled into the capsule package and sealed. Previous work has demonstrated passive localization using Eudragit polymers to deliver sensors to the small intestines[46] and has validated the device's signal integrity by maintaining communication up to 72 cm away from simulated abdominal muscle and tissue.[15] Following assembly, the ingestible device was submerged in PBS to confirm sensor readout and device communication in fluid. The ingestible device was evaluated in SIF at 37°C after exposure to SGF to confirm package integrity and sensor stability in simulated GI conditions (Figure 4C). Similar to the characterization of the PEDOT:PSS sensor in NaCl solution, the SIF solution was spiked to physiologically relevant ionic concentrations ranging from 150 to 200 mM. After 2.5 h exposure to SGF, the entire device was submerged in SIF (Figure 4D) and connected to a smartphone via a BLE app (SI Connect, Silicon Labs, Austin, TX, USA). Real-time impedance data were recorded and wirelessly transmitted to the smartphone every minute for 5 s. Liu et al.[47] reported a capsule propagation velocity due to peristalsis of 1–2 cm/min, making the sampling rate suitable for centimeter-resolution spatial monitoring in the small intestine. The ingestible device captured the magnitude impedance change as the SIF concentration was increased every 3 min, yielding a sensitivity of −2.7 Ω/mM with an average 0.87 Ω/mM error at each concentration interval (Figure 4E). These results successfully demonstrate continuous measurement in simulated GI conditions with low variability, suitable for *in vivo* operation.

Ex vivo validation of the device on mouse colonic tissue

Simulated GI fluids and mock tissue models are commonly used for preliminary evaluation of ingestible device performance in the GI tract,[48] simulating some mechanical and chemical properties of the intestinal environment. However, these *in vitro* methods cannot replicate the enhanced mucosal permeability associated with inflammation, necessitating the use of accurate animal models to replicate inflamed intestinal tissue. To mimic inflamed tissues *ex vivo*, inducible intestinal epithelial damage and TJ dilation are modeled in excised animal tissue using acetic-acid-induced methods and EDTA-chelating agents.[49,50] To validate its functionality, the capsule device was tested *ex vivo* on excised mouse colonic tissues with varying levels of permeability, emulating the effects of inflammation on epithelial barrier function. Calcium directly interacts with the adherens junction protein E-cadherin and indirectly regulates TJ proteins. Removal of extracellular calcium can disrupt TJ function, increasing paracellular permeability.[51] Here, EDTA is used to enhance mucosal permeability through calcium chelation.[52] By controlling the dosage and exposure time of EDTA, the permeability and dilation of TJs can be regulated (Figure 5A).[53] The testing protocol, adapted from Holt et al.,[35] starts with a wireless baseline tissue impedance measurement via the bioimpedance-sensing capsule (Figure 5B). Subsequently, the tissue is exposed for 1 min under varying EDTA concentrations (1, 3, 5, and 10 mM). Between exposures, bioimpedance data are captured and logged wirelessly. Previous work confirmed the EDTA exposure protocol varied permeability levels of colonic tissue via TEER measurements in a Ussing chamber,[35] demonstrating an increase in tissue conductivity with higher-dosage EDTA exposure. Here, bioimpedance measurements were taken on excised mouse colon tissue (N = 6) (Figure 5C), yielding 70% and 50% reductions in relative tissue impedance after exposure to 3 and 10 mM EDTA, respectively (Figure 5D). Measurements verified that the ingestible device can reliably quantify mucosal permeability through the dilation of TJs induced by calcium chelation. Since TJ dilation is a key mechanism in the manifestation of IBD,[54] this result signified a key step toward monitoring inflammation by quantifying permeability using a bioimpedance-sensing capsule.

In vivo characterization of the device in a rat colitis model

While EDTA treatment of *ex vivo* mouse tissue was observed to enhance tissue permeability, mimicking the effects of inflammation on TJ function, it does not emulate changes in morphology, immune response, and the physiological environment of IBD. Alternatively, inducing injury in live animal models provides an *in vivo* model for the clinical manifestation of inflammation. IBD-like injuries are induced by administering chemical agents such as acetic acid, indomethacin, and dextran sodium sulfate (DSS).[55] These inflamed animal models provide a setting for evaluating mucosal permeability under conditions that mimic the IBD pathophysiology. DSS-induced colitis in rats is an established animal model that mimics the epithelial barrier disruption and triggers an inflammatory response similar to that seen in human ulcerative colitis, a form of IBD.[56,57] Thus, DSS-induced colitis provides a reliable model to assess mucosal permeability and disease activity index (DAI) *in vivo*.[57]

In vivo evaluation of the bioimpedance-sensing capsule was accomplished by surgically implanting it in the rat cecum and wirelessly measuring bioimpedance in various colitis disease states. Colitis was induced by administering a 6% DSS solution as drinking water for 5 days. Body weight and DAI were monitored during and after DSS administration to confirm the progression of colitis. The DSS-treated rats showed a peak decrease of 6.7% in body weight (Figure 6A) and exhibited elevated stool consistency (Figure 6B) and overall DAI scores (Figure 6C) compared with the control groups. These DAI metrics provide a quantitative measure of the disease severity, which serves as a benchmark for validating the bioimpedance device's ability to detect inflammation-associated changes in tissue conductivity.[35,56,57]

Inflammatory processes in DSS-induced colitis disrupt ion transport channels and TJ integrity, resulting in increased tissue conductivity.[58] To evaluate colitis progression, we measured cecum bioimpedance at subclinical (day 4 of DSS treatment, N = 5 per group) and peak inflammation (day 8 post-DSS administration, N = 5 per group) time points in the treated and control rat groups (Figure S4). Altered permeability was inferred from changes in bioimpedance, which was recorded *in vivo* using a fully assembled bioimpedance-sensing capsule implanted in the cecum of each rat (Figure 6D). EIS measurements were taken from 100 Hz to 200 kHz for 60 s. The average bioimpedance

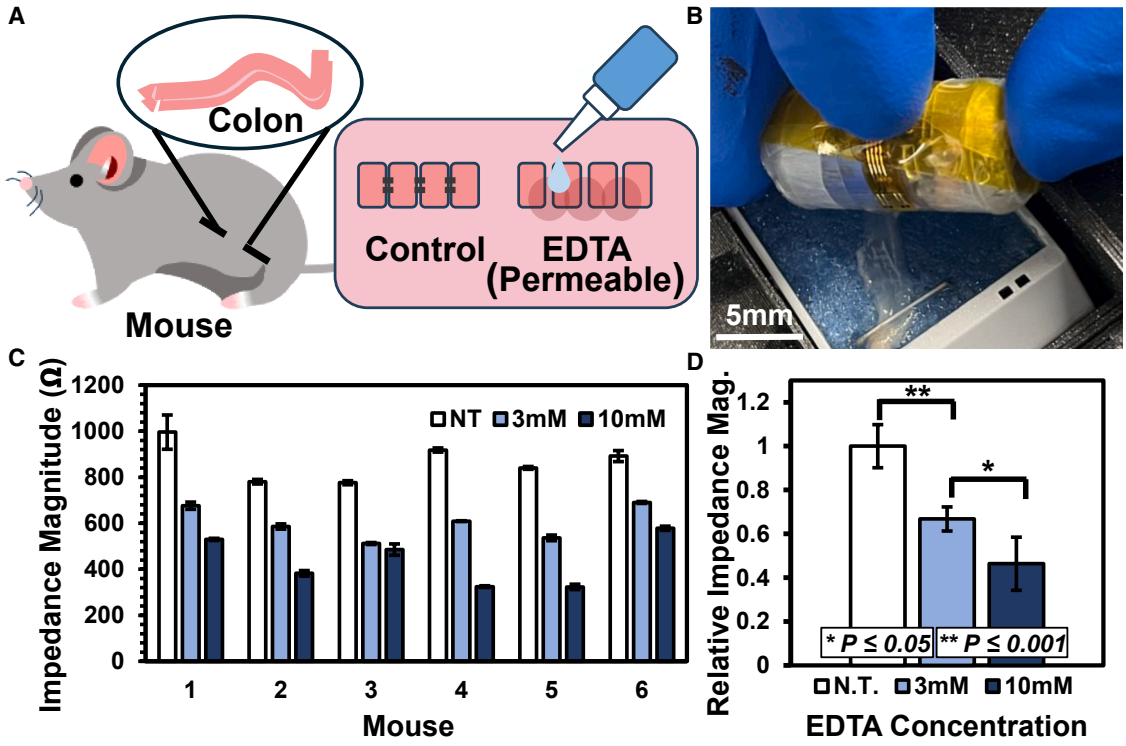

Figure 5. *Ex vivo* mouse study

(A) EDTA treatment of mouse colonic tissue.

(B) Image of assembled capsule next to excised mouse tissue.

(C) Impedance magnitude at 10 kHz collected wirelessly by the capsule placed on tissue from $N = 6$ mice at a non-treated (NT) control concentration and at 3 and 10 mM EDTA concentrations.

(D) Average impedance magnitude across all mice at 10 kHz plotted relative to the magnitude before EDTA treatment.

Error bars shown as standard deviation (SD) of mean.

magnitudes in cecal tissue demonstrate a measurable difference between control, early subclinical, and peak inflammation colitis models. A 10 kHz interrogation frequency demonstrated stable quantification of mucosal permeability,[35] allowing the sensor to detect changes in conductivity from TJ dilation. Compared with the control measurements, average reductions of 23% and 60% in cecal impedance were observed for the subclinical model stage and peak inflammation models, respectively (Figure 6E). There is a large variance of 28%, 36%, and 36% for control, early-onset, and peak inflammation measurements, most likely due to variable physiological factors such as animal size, disease severity, and electrode contact pressure when implanted. Following bioimpedance measurements, the rats were euthanized, and cecum tissue was collected for hematoxylin and eosin (H&E) staining and histological analysis. Figures 6F–6H depict histological images of the rat cecum in the different measurement groups. Control tissue histology shows a healthy epithelial lining with structured crypts. Histology on day 4 in the DSS-administered group also shows no signs of inflammation, consistent with measurements between control and DSS groups, where measurement differences were not statistically significant. Histological analysis from peak inflammation shows signs of microscopic inflammation in immune cell infiltration and minor epithelial damage but no macroscopic inflammatory signs. Likewise, the ingestible device detected a significant difference in bioimpedance magnitude between the control and DSS groups at the peak inflammation stage, with minor histological injury. Bioimpedance measurements agree with histological analysis results, validating the device's ability to detect microscopic inflammation *in vivo* in rat colitis models.

These results represent a significant step toward the realization of an ingestible device for real-time, spatially resolute monitoring of inflammation throughout the GI tract. Future work with large-animal models, such as pigs, would enable longitudinal monitoring of IBD progression using bioimpedance capsule devices. Large-animal models will directly interrogate how external forces from peristalsis can cause measurement variability and contact issues,[59] which were not present in this controlled *in vivo* study. Translation of this device to a large-animal model requires further miniaturization to comply with the US FDA standards of a 000 pill size (26 × 10 mm).[12] In a clinical setting, we anticipate that this technology would require baseline calibration for each patient to account for variability in the bioimpedance readout. Periodic measurement with the noninvasive device could then be performed to track changes in permeability throughout the GI tract in response to therapeutics or to detect potential IBD flare-ups before they become severe. Additionally, multiple sensors could be packaged around the capsule to ensure a point of

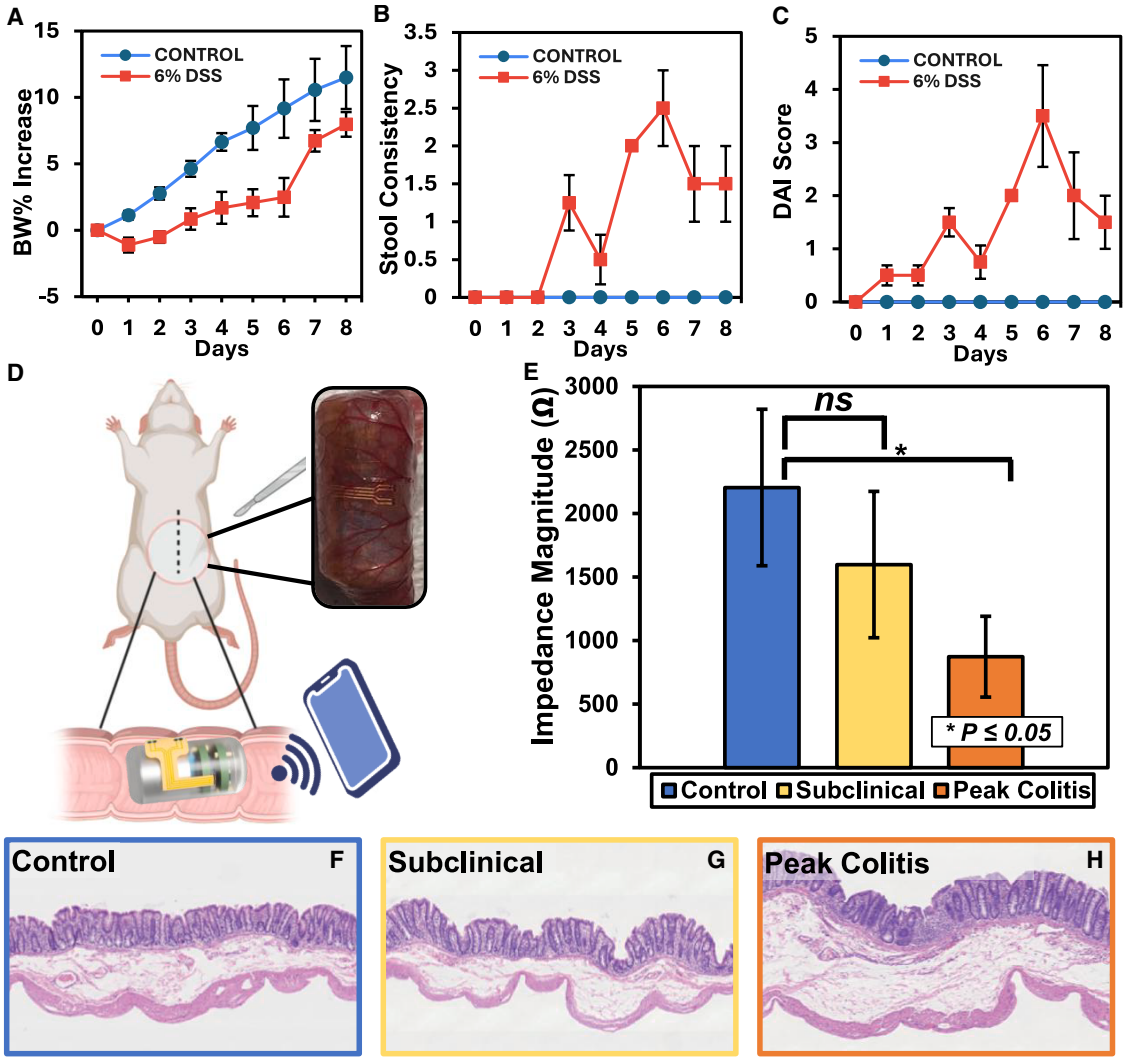

Figure 6. *In vivo* rat study

(A) Body weight percentage increase of control vs. DSS treatment rats.
(B) Stool consistency of control vs. DSS treatment rats.
(C) Disease activity index (DAI) score of control vs. DSS treatment rats.
(D) Overview of rat surgery and capsule implantation.
(E) *In vivo* cecal bioimpedance measurement average of the control group ($N = 6$) and subclinical and peak inflammation ($N = 5$).
(F–H) Histological analysis of control, subclinical, and peak colitis models, respectively.
Error bars shown as standard deviation (SD) of mean.

contact for continuous, reliable bioimpedance measurement. With a combination of device miniaturization and addressing sensor contact through additional sensors, a bioimpedance ingestible device can be realized for IBD monitoring in large-animal models toward its use in a clinical setting.

Conclusion

This work introduces a novel bioimpedance-sensing capsule for *in vivo* evaluation of mucosal permeability, providing a platform for studying GI pathophysiology in rodent colitis models. Electropolymerized PEDOT:PSS electrodes improve CSC 375-fold over Au sensors; this is a 7.3-fold increase over previous electrodeposition methods. Testing in simulated GI fluids verifies package stability after physiologically relevant transit times and demonstrates minimal sensor drift suitable for measurement during GI transit. Mucosal permeability is quantified *ex vivo* in mouse colon tissue, validating the device's ability to differentiate tissue based on permeability. Bioimpedance is measured wirelessly *in vivo* in a DSS-induced rat colitis model by implanting the ingestible device into the rat cecum. Reductions of 23% and 60% in average cecal bioimpedance at the subclinical and peak stages of inflammation, respectively, demonstrate the device's ability to detect and differentiate inflammation during the progression of IBD. Histological analysis

Please cite this article in press as: Lim et al., *In vivo* monitoring of tissue permeability in a rat colitis model via a bioimpedance-sensing ingestible device, Device (2026), https://doi.org/10.1016/j.device.2026.101180

supports this claim, showing no visible signs of inflammation at the subclinical stage and mild histological injury at peak cecal inflammation. This is a significant step toward early-stage monitoring of IBD using subclinical biomarkers that are not optically visible. Bioimpedance sensing could also be used to monitor recovery from disease and quantify treatment response. Further progression of this work would involve testing the device during complete GI transit through a large-animal model, such as a porcine model. Large IBD animal models would allow inflammation to be monitored through the ingestible device at multiple stages of IBD progression, including recovery. However, translating this work to achieve complete GI transit requires investigation of interfering conditions such as peristalsis, tissue contact, chemical and biological interferants, and device size. Bioimpedance sensing offers a promising sensing modality for detecting and localizing areas of inflammation before IBD progression exacerbates these symptoms. Furthermore, bioimpedance sensing enables feedback-driven operation in autonomous applications such as biopsy and drug delivery, thereby improving diagnostic and treatment efficacy. Future work will focus on integrating additional sensor modalities, such as pH, to improve regional localization within the GI tract, incorporating multiple bioimpedance sensors distributed radially around the capsule to enhance spatial resolution, and introducing pressure sensors to detect contact events between the device and surrounding tissue to enhance therapeutic applications. Overall, advancements in bioimpedance-sensing ingestible devices make significant strides toward noninvasive localization of inflammation and early-stage monitoring of IBD. Although not yet approved for clinical use, this work shows a significant advancement in bioimpedance capsule technology for *in vivo* monitoring of tissue permeability in animal models.

METHODS

Bioimpedance sensor fabrication

Four-probe flexible bioimpedance sensors (with a 500 μm electrode width and 1 mm spacing) were fabricated onto 1-Mil Kapton polyimide film (DuPont, Wilmington, DE, USA). Traces were patterned with Shipley S1813 photoresist (Kayaku Advanced Materials, Westborough, MA, USA) using an MLA150 Maskless Aligner (Heidelberg Instruments, Heidelberg, Germany), followed by deposition of Cr/Au (20/200 nm) using electron-beam evaporation and lift-off with acetone for 15 min under sonication. The substrate was coated with 1.6 μm of Parylene-C to insulate Au traces from the external environment. Electrodes and contact pads were exposed by RIE with 100 SCCM O_2 (at 100 mTorr) for 300 s at 50 W using a Trion RIE (Trion Technology, Clearwater, FL, USA). Sensors were cleaned with acetone, methanol, and isopropanol (AMI), rinsed thoroughly with deionized water (>18.2 MΩ), and dried with N_2. Au electrodes were coated with a PEDOT:PSS film via CP using a BioLogic VSP300 potentiostat (current density: 5 $\mu A/mm^2$) for 180 s in a solution of 10 mM EDOT and 2% w/v PSS.

PEDOT:PSS electrode characterization

CV using a BioLogic VSP300 potentiostat (−0.5 to +0.5 V; 100 mV/s) was used to characterize the CSC of the sensing electrodes before and after electropolymerization of PEDOT:PSS. Integration of the output cyclic voltammogram over the scan rate yielded the CSC of the electrodes (C/m^2). A Phenom XL scanning electron microscope (Thermo Fisher Scientific) was used to take images of electrodes (3,100× magnification; 10 kV; 0.10 Pa).

Capsule electronics and assembly

PCB electronics feature an analog front-end (AFE) IC, AD5941 (Analog Devices), for performing EIS; a BLE microcontroller (BLE-MCU), BGM13S (Silicon Labs), for data processing and wireless communication; and a magnetic reed switch, HSR-502RT (Hermetic Switch), connected between the battery and PCB. The capsule shell (⌀ = 14 mm) is LCD 3D printed from surgical guide resin (Formlabs). Bioimpedance sensors are inserted through a 1-mm port on the side of the capsule shell and connected to the AFE via a 4-pin FFC (pitch: 0.5 mm). The port and capsule ends are sealed with surgical guide resin and cured for 30 s using an LED UV curing system (UV75 Curing Light, Thorlabs, Newton, NJ, USA).

Bioimpedance measurement via the ingestible device

The ingestible capsule communicates with the SI Connect mobile application via the BGM13S MCU (Silicon Labs) over a Bluetooth 5.1 connection. Bidirectional read and write functionality allows wireless programming of the onboard electronics to optimize excitation parameters (e.g., frequency sweep or single frequency operation, voltage amplitude, and frequency range) and to initiate EIS measurements remotely. To perform four-wire impedance measurements, the AD5941 AFE (Analog Devices) uses an integrated high-speed digital-to-analog converter (DAC) to generate the AC excitation signal, while a transimpedance amplifier (TIA) measures the resulting current response. The excitation signal is a 100-mV_{p-p} sinusoidal waveform with a frequency sweep range from 100 Hz to 200 kHz, sampled at 50 points per decade. A 1-kΩ resistor is placed in series to limit the current delivered to the tissue. Current is injected through the two outer electrodes, and the resulting voltage difference is measured across two inner electrodes. The sensed voltage readout is stabilized by an internal low-pass TIA filter and digitized by a 16-bit ADC. The AD5941 uses an internal discrete Fourier transform (DFT) hardware accelerator to compute impedance magnitude and phase. The BGM13S MCU polls for interrupts every 100 ms. When data are available, the AD5941 AFE triggers an interrupt, prompting the MCU to retrieve measurement data via a serial peripheral interface (SPI) and transmit it wirelessly to the mobile device. No external signal conditioning was performed.

EDTA challenge on mouse colonic tissue

Colonic tissue is extracted from a C57BL/6 mouse and preserved in Krebs-Ringer Bicarbonate (KRB) buffer oxygenated with carbogen gas (95% O_2, 5% CO_2). Before each measurement, the tissue sample was sequentially submerged in the EDTA+KRB mixture (at 1, 3, 5, and 10 mM) for 1 min and fixed to a biopsy sponge. The sensor-integrated capsule was placed on the tissue, and EIS was performed from 100 Hz to 100 kHz, with wireless data sent to a smartphone via Bluetooth.

Experimental design of DSS challenge in the rat colitis model

All animal procedures were conducted in accordance with the University of Maryland Institutional Animal Care and Use Committee (IACUC) guidelines under the approved protocol #R-JUL-24-24. DSS with a relative molecular weight of 40,000 (Cayman Chemical, Ann Arbor, MI, USA, cat. no. 23250-100) and 10% formalin (VWR, Radnor, PA, USA, cat. no. 16004-128) were purchased for the rat colitis study. Upon arrival, 8-week-old white rats (*Rattus norvegicus*) were randomly assigned to DSS-treated or non-treated control groups, with eight rats per group ($N = 16$). Following a 7-day acclimatization period, colitis was induced in the DSS treatment group by administering 6% DSS in drinking water for 5 consecutive days, followed by a 3-day recovery period with normal water. The severity of colitis was monitored daily using body weight, DAI, and stool consistency scores, as previously described.[60] DAI scores were calculated by summing three metrics at each time point: weight loss (0: <1%, 1: 1%–5%, 2: 5%–10%, 3: 10%–15%, and 4: >15%), stool consistency (0: no diarrhea, 2: loose stool not adhering to the anus, and 4: liquid stool adhering to the anus), and fecal blood (0: none, 2: moderate, and 4: gross bleeding).

Caecum permeability and bioimpedance measurement

The bioimpedance capsules were surgically implanted into the cecum of colitis ($N = 8$) and control ($N = 8$) rats under anesthesia. To quantify colitis progression from early-stage to peak inflammation, EIS measurements (100 Hz–200 kHz, 50 mV_{p-p}) repeated over 60 s were conducted on days 4 ($N = 8$) and 8 ($N = 8$). EIS measurements are wirelessly initiated by external commands sent to the ingestible capsule using BLE and the Si Connect mobile app. The EIS spectrum was generated using a 50 mV small-amplitude AC voltage signal with frequencies ranging from 100 Hz to 200 kHz (ten frequencies per decade). Between each implantation surgery, the ingestible capsule was briefly placed on a neodymium magnet to open the reed switch, disconnecting the device and conserving battery power when not in use. Data sent to the external BLE device were imported into MATLAB (MathWorks, Natick, MA, USA) for parsing and analysis.

Histopathological analysis

For histological analysis with H&E staining, caecum samples were collected from both groups on days 4 and 8. The tissues were dissected longitudinally, rinsed with 1× PBS, and gently sandwiched between form pads in cassettes before overnight fixation in 10% formalin solution. The fixed tissues were then transferred to a 70% ethanol solution, dehydrated, and embedded in paraffin wax. Sections were cut at 4 μM, mounted on glass slides, and stained with H&E for histopathological assessment.

Statistical analysis

CV was performed before and after electropolymerization, and integration was performed on (i/v) curves to calculate CSC. The standard deviation (SD) for $N = 3$ sensors is used to evaluate the reproducibility of the electropolymerization process. For *ex vivo* mouse testing, a paired *t* test was employed to assess the average magnitude differences ($N = 6$). All rat data were statistically analyzed by GraphPad Prism 10 and are presented as mean ± SEM ($N = 8$). Group comparisons were performed using two-way ANOVA with repeated time-point measurements, and the statistical significance was defined as $p < 0.05$. The Sidak post hoc test was applied for multiple comparisons.

RESOURCE AVAILABILITY

Lead contact

Requests for further information and resources should be directed to and will be fulfilled by the lead contact, Reza Ghodssi (ghodssi@umd.edu).

Materials availability

This study did not generate new unique reagents.

Data and code availability

The data that support the findings of this study are available in the supplemental information (Data S2). Additional data reported in this paper are available from the lead contact upon request.

ACKNOWLEDGMENTS

This work was supported by the TEDCO Maryland Innovation Initiative (MII) award. The authors would like to thank the University of Maryland NanoCenter FabLab and the Department of Laboratory Animal Resources for their assistance.

AUTHOR CONTRIBUTIONS

M.W.L., J.M.S., Y.J., and R.G. were responsible for conceiving the research. J.M.S. designed the ingestible device electronics. M.W.L. and J.M.K. carried out the device fabrication and characterization. H.A. and Y.J. designed the *ex vivo* and *in vivo* studies and carried out the experiments with assistance from M.W.L. in operating the device. M.W.L. and H.A. performed the data analysis. M.W.L., H.A., and J.M.S. wrote the original draft of the manuscript. M.W.L., H.A., J.M.S., Y.J., and R.G. participated in reviewing and editing the manuscript. R.G. and J.M.S. acquired funding for the project. J.M.S., Y.J., and R.G. supervised the research.

DECLARATION OF INTERESTS

We, the authors, have a non-provisional patent application related to this work: J.M. Stine, L.A. Beardslee, R. Ghodssi, P.J. Pasricha, J.A. Levy, M.A. Straker, B. Holt, V. Borbash, H. Abianeh, "Bioimpedance Sensor-integrated Capsule for Monitoring," US non-provisional application no. 18/329533, filed on June 5, 2023.

SUPPLEMENTAL INFORMATION

Supplemental information can be found online at https://doi.org/10.1016/j.device.2026.101180.

Received: March 9, 2026
Revised: May 1, 2026
Accepted: May 5, 2026

REFERENCES

1. Ng, S.C., Shi, H.Y., Hamidi, N., Underwood, F.E., Tang, W., Benchimol, E.I., Panaccione, R., Ghosh, S., Wu, J.C.Y., Chan, F.K.L., et al. (2017). Worldwide incidence and prevalence of inflammatory bowel disease in the 21st century: a systematic review of population-based studies. Lancet *390*, 2769–2778. https://doi.org/10.1016/S0140-6736(17)32448-0.

2. Qiao, Y., He, C., Xia, Y., Ocansey, D.K.W., and Mao, F. (2025). Intestinal mucus barrier: A potential therapeutic target for IBD. Autoimmun. Rev. *24*, 103717. https://doi.org/10.1016/j.autrev.2024.103717.
3. McGuckin, M.A., Eri, R., Simms, L.A., Florin, T.H.J., and Radford-Smith, G. (2009). Intestinal Barrier Dysfunction in Inflammatory Bowel Diseases. Inflamm. Bowel Dis. *15*, 100–113. https://doi.org/10.1002/ibd.20539.
4. Ahmed, M. (2022). Video Capsule Endoscopy in Gastroenterology. Gastroenterol. Res. *15*, 47–55. https://doi.org/10.14740/gr1487.
5. Feakins, R.M.; British Society of Gastroenterology (2013). Inflammatory bowel disease biopsies: updated British Society of Gastroenterology reporting guidelines. J. Clin. Pathol. *66*, 1005–1026. https://doi.org/10.1136/jclinpath-2013-201885.
6. Bencardino, S., D'Amico, F., Zilli, A., Parigi, T.L., Allocca, M., Fiorino, G., Danese, S., and Furfaro, F. (2024). Fecal, Blood, and Urinary Biomarkers in Inflammatory Bowel Diseases. J. Transl. Gastroenterol. *2*, 61–75. https://doi.org/10.14218/JTG.2024.00001.
7. Srinivasan, B., Kolli, A.R., Esch, M.B., Abaci, H.E., Shuler, M.L., and Hickman, J.J. (2015). TEER measurement techniques for in vitro barrier model systems. J. Lab. Autom. *20*, 107–126. https://doi.org/10.1177/2211068214561025.
8. Weijenborg, P.W., Rohof, W.O.A., Akkermans, L.M.A., Verheij, J., Smout, A.J.P.M., and Bredenoord, A.J. (2013). Electrical tissue impedance spectroscopy: a novel device to measure esophageal mucosal integrity changes during endoscopy. Neuro Gastroenterol. Motil. *25*, 574.e458. https://doi.org/10.1111/nmo.12106.
9. Wegener, J., Keese, C.R., and Giaever, I. (2000). Electric Cell–Substrate Impedance Sensing (ECIS) as a Noninvasive Means to Monitor the Kinetics of Cell Spreading to Artificial Surfaces. Exp. Cell Res. *259*, 158–166. https://doi.org/10.1006/excr.2000.4919.
10. Khoshbin, K., Khanna, L., Maselli, D., Atieh, J., Breen-Lyles, M., Arndt, K., Rhoten, D., Dyer, R.B., Singh, R.J., Nayar, S., et al. (2021). Development and Validation of Test for "Leaky Gut" Small Intestinal and Colonic Permeability Using Sugars in Healthy Adults. Gastroenterology *161*, 463–475.e13. https://doi.org/10.1053/j.gastro.2021.04.020.
11. Rao, A.S., Camilleri, M., Eckert, D.J., Busciglio, I., Burton, D.D., Ryks, M., Wong, B.S., Lamsam, J., Singh, R., and Zinsmeister, A.R. (2011). Urine sugars for in vivo gut permeability: validation and comparisons in irritable bowel syndrome-diarrhea and controls. Am. J. Physiol. Gastrointest. Liver Physiol. *301*, G919–G928. https://doi.org/10.1152/ajpgi.00168.2011.
12. Thwaites, P.A., Yao, C.K., Halmos, E.P., Muir, J.G., Burgell, R.E., Berean, K.J., Kalantar-zadeh, K., and Gibson, P.R. (2024). Review article: Current status and future directions of ingestible electronic devices in gastroenterology. Aliment. Pharmacol. Ther. *59*, 459–474. https://doi.org/10.1111/apt.17844.
13. Cheng, C., Wu, Y., Li, X., An, Z., Lu, Y., Zhang, F., Su, B., and Liu, Q. (2021). A wireless, ingestible pH sensing capsule system based on iridium oxide for monitoring gastrointestinal health. Sens. Actuators B Chem. *349*, 130781. https://doi.org/10.1016/j.snb.2021.130781.
14. van der Schaar, P.J., Dijksman, J.F., Broekhuizen-de Gast, H., Shimizu, J., van Lelyveld, N., Zou, H., Iordanov, V., Wanke, C., and Siersema, P.D. (2013). A novel ingestible electronic drug delivery and monitoring device. Gastrointest. Endosc. *78*, 520–528. https://doi.org/10.1016/j.gie.2013.03.170.
15. Stine, J.M., Ruland, K.L., Beardslee, L.A., Levy, J.A., Abianeh, H., Botasini, S., Pasricha, P.J., and Ghodssi, R. (2024). Miniaturized Capsule System Toward Real-Time Electrochemical Detection of H2S in the Gastrointestinal Tract. Adv. Healthc. Mater. *13*, 2302897. https://doi.org/10.1002/adhm.202302897.
16. Even, A., Minderhoud, R., Torfs, T., Leonardi, F., van Heusden, A., Sijabat, R., Firfilionis, D., Castro Miller, I.D., Rammouz, R., Teichmann, T., et al. (2025). Measurements of redox balance along the gut using a miniaturized ingestible sensor. Nat. Electron. *8*, 856–870. https://doi.org/10.1038/s41928-025-01411-4.
17. Chen, J., Alexiev, A., Sergnese, A., Fabian, N., Pettinari, A., Cai, Y., Perepelook, V., Schmidt, K., Hayward, A., Guevara, A., et al. (2025). An ingestible capsule for luminance-based diagnosis of mesenteric ischemia. Sci. Robot. *10*, eadx1367. https://doi.org/10.1126/scirobotics.adx1367.
18. Son, D., Gilbert, H., and Sitti, M. (2020). Magnetically Actuated Soft Capsule Endoscope for Fine-Needle Biopsy. Soft Robot. *7*, 10–21. https://doi.org/10.1089/soro.2018.0171.
19. Kim, K., Edwards, S., Fuxa, K., Lin, H., Shrestha, S., Fan, H., Diaz, N., Berinstein, J., Naik, R., Zhou, Y., and Dong, X. (2025). Mucosa-Interfacing Capsule for In Situ Sensing the Elasticity of Biological Tissues. Adv. Mater. Technol. *10*, 2401487. https://doi.org/10.1002/admt.202401487.
20. Chiang, S., Eschbach, M., Knapp, R., Holden, B., Miesse, A., Schwaitzberg, S., and Titus, A. (2021). Electrical impedance characterization of in vivo porcine tissue using machine learning. J. Electr. Bioimpedance *12*, 26–33. https://doi.org/10.2478/joeb-2021-0005.
21. Kassanos, P. (2021). Bioimpedance Sensors: A Tutorial. IEEE Sens. J. *21*, 22190–22219. https://doi.org/10.1109/JSEN.2021.3110283.
22. Bertemes-Filho, P., and Morcelles, K.F. (2022). Wearable Bioimpedance Measuring Devices. In Medicine-Based Informatics and Engineering, F. Simini and P. Bertemes-Filho, eds. (Springer International Publishing), pp. 81–101. https://doi.org/10.1007/978-3-030-87845-0_5.
23. Zhang, J., Balakrishnan, G., Srinidhi, S., Bhat, A., Kumar, S., and Bettinger, C. (2023). NFCapsule: An Ingestible Sensor Pill for Eosinophilic Esophagitis Detection Based on near-Field Coupling. In Proceedings of the 20th ACM Conference on Embedded Networked Sensor Systems SenSys '22 (Association for Computing Machinery)), pp. 75–90. https://doi.org/10.1145/3560905.3568523.
24. Balakrishnan, G., Bhat, A., Naik, D., Kim, J.S., Marukyan, S., Gido, L., Ritter, M., Khair, A.S., and Bettinger, C.J. (2023). Gelatin-Based Ingestible Impedance Sensor to Evaluate Gastrointestinal Epithelial Barriers. Adv. Mater. *35*, 2211581. https://doi.org/10.1002/adma.202211581.
25. Štukovnik, Z., and Bren, U. (2022). Recent Developments in Electrochemical-Impedimetric Biosensors for Virus Detection. Int. J. Mol. Sci. *23*, 15922. https://doi.org/10.3390/ijms232415922.
26. Franks, W., Schenker, I., Schmutz, P., and Hierlemann, A. (2005). Impedance characterization and modeling of electrodes for biomedical applications. IEEE Trans. Biomed. Eng. *52*, 1295–1302. https://doi.org/10.1109/TBME.2005.847523.
27. Desai, S.A., Rolston, J.D., Guo, L., and Potter, S.M. (2010). Improving impedance of implantable microwire multi-electrode arrays by ultrasonic electroplating of durable platinum black. Front. Neuroeng. *3*, 5. https://doi.org/10.3389/fneng.2010.00005.
28. Gabriel, G., Gómez-Martínez, R., and Villa, R. (2008). Single-walled carbon nanotubes deposited on surface electrodes to improve interface impedance. Physiol. Meas. *29*, S203–S212. https://doi.org/10.1088/0967-3334/29/6/S18.
29. Boehler, C., Oberueber, F., Schlabach, S., Stieglitz, T., and Asplund, M. (2017). Long-Term Stable Adhesion for Conducting Polymers in Biomedical Applications: IrOx and Nanostructured Platinum Solve the Chronic Challenge. ACS Appl. Mater. Interfaces *9*, 189–197. https://doi.org/10.1021/acsami.6b13468.
30. Benoudjit, A., Bader, M.M., and Wan Salim, W.W.A. (2018). Study of electropolymerized PEDOT:PSS transducers for application as electrochemical sensors in aqueous media. Sens. Biosensing. Res. *17*, 18–24. https://doi.org/10.1016/j.sbsr.2018.01.001.
31. Abu-Saude, M., and Morshed, B.I. (2018). Characterization of a Novel Polypyrrole (PPy) Conductive Polymer Coated Patterned Vertical CNT (pvCNT) Dry ECG Electrode. Chemosensors *6*, 27. https://doi.org/10.3390/chemosensors6030027.
32. Green, R.A., Lovell, N.H., Wallace, G.G., and Poole-Warren, L.A. (2008). Conducting polymers for neural interfaces: Challenges in developing an effective long-term implant. Biomaterials *29*, 3393–3399. https://doi.org/10.1016/j.biomaterials.2008.04.047.

33. Steiger, C., Abramson, A., Nadeau, P., Chandrakasan, A.P., Langer, R., and Traverso, G. (2019). Ingestible electronics for diagnostics and therapy. Nat. Rev. Mater. *4*, 83–98. https://doi.org/10.1038/s41578-018-0070-3.

34. Barducci, L., Norton, J.C., Sarker, S., Mohammed, S., Jones, R., Valdastri, P., and Terry, B.S. (2020). Fundamentals of the gut for capsule engineers. Prog. Biomed. Eng. *2*, 042002. https://doi.org/10.1088/2516-1091/abab4c.

35. Holt, B.M., Stine, J.M., Beardslee, L.A., Ayansola, H., Jin, Y., Pasricha, P.J., and Ghodssi, R. (2025). An ingestible bioimpedance sensing device for wireless monitoring of epithelial barriers. Microsyst. Nanoeng. *11*, 24. https://doi.org/10.1038/s41378-025-00877-8.

36. Kassanos, P., Seichepine, F., and Yang, G.-Z. (2019). Characterization and Modeling of a Flexible Tetrapolar Bioimpedance Sensor and Measurements of Intestinal Tissues. In 2019 IEEE 19th International Conference on Bioinformatics and Bioengineering (BIBE), pp. 686–690. https://doi.org/10.1109/BIBE.2019.00129.

37. Lee, E.K., Baruah, R.K., Bhamra, H., Kim, Y.-J., and Yoo, H. (2021). Recent advances in electrode development for biomedical applications. Biomed. Eng. Lett. *11*, 107–115. https://doi.org/10.1007/s13534-021-00189-6.

38. Hassibi, A., Navid, R., Dutton, R.W., and Lee, T.H. (2004). Comprehensive study of noise processes in electrode electrolyte interfaces. J. Appl. Phys. *96*, 1074–1082. https://doi.org/10.1063/1.1755429.

39. Schander, A., Strokov, S., Stemmann, H., Teßmann, T., Kreiter, A.K., and Lang, W. (2019). A Flexible 202-Channel Epidural ECoG Array With PEDOT: PSS Coated Electrodes for Chronic Recording of the Visual Cortex. IEEE Sens. J. *19*, 820–825. https://doi.org/10.1109/JSEN.2018.2880833.

40. Zabihi, F., Xie, Y., Gao, S., and Eslamian, M. (2015). Morphology, conductivity, and wetting characteristics of PEDOT:PSS thin films deposited by spin and spray coating. Appl. Surf. Sci. *338*, 163–177. https://doi.org/10.1016/j.apsusc.2015.02.128.

41. Starbird, R., Bauhofer, W., Meza-Cuevas, M., and Krautschneider, W.H. (2012). Effect of experimental factors on the properties of PEDOT-NaPSS galvanostatically deposited from an aqueous micellar media for invasive electrodes. In The 5th 2012 Biomedical Engineering International Conference (IEEE), pp. 1–5. https://doi.org/10.1109/BMEiCon.2012.6465500.

42. Kiela, P.R., and Ghishan, F.K. (2016). Physiology of Intestinal Absorption and Secretion. Best Pract. Res. Clin. Gastroenterol. *30*, 145–159. https://doi.org/10.1016/j.bpg.2016.02.007.

43. O'Grady, J., Murphy, C.L., Barry, L., Shanahan, F., and Buckley, M. (2020). Defining gastrointestinal transit time using video capsule endoscopy: a study of healthy subjects. Endosc. Int. Open *8*, E396–E400. https://doi.org/10.1055/a-1073-7653.

44. FDA (2024). Ingestible Telemetric Gastrointestinal Capsule Imaging System - Final Class II Special Controls Guidance Document for Industry and FDA (FDA).

45. Abdigazy, A., Arfan, M., Lazzi, G., Sideris, C., Abramson, A., and Khan, Y. (2024). End-to-end design of ingestible electronics. Nat. Electron. *7*, 102–118. https://doi.org/10.1038/s41928-024-01122-2.

46. Banis, G.E., Beardslee, L.A., Stine, J.M., Sathyam, R.M., and Ghodssi, R. (2020). Capacitive sensing of triglyceride film reactions: a proof-of-concept demonstration for sensing in simulated duodenal contents with gastrointestinal targeting capsule system. Lab Chip *20*, 2020–2032. https://doi.org/10.1039/D0LC00133C.

47. Liu, L., Towfighian, S., and Hila, A. (2015). A Review of Locomotion Systems for Capsule Endoscopy. IEEE Rev. Biomed. Eng. *8*, 138–151. https://doi.org/10.1109/RBME.2015.2451031.

48. Dixit, Y., Kanojiya, K., Bhingardeve, N., Ahire, J.J., and Saroj, D. (2024). In Vitro Human Gastrointestinal Tract Simulation Systems: A Panoramic Review. Probiotics Antimicrob. Proteins *16*, 501–518. https://doi.org/10.1007/s12602-023-10052-y.

49. Ventrella, D., Salaroli, R., Elmi, A., Carnevali, G., Forni, M., Baldi, F., and Bacci, M.L. (2020). A novel ex vivo porcine model of acid-induced esophageal damage for preliminary functional evaluations of anti-gastroesophageal reflux disease medical devices. Vet. World *13*, 2728–2735. https://doi.org/10.14202/vetworld.2020.2728-2735.

50. Marrero, D., Guimera, A., Maes, L., Villa, R., Alvarez, M., and Illa, X. (2023). Organ-on-a-chip with integrated semitransparent organic electrodes for barrier function monitoring. Lab Chip *23*, 1825–1834. https://doi.org/10.1039/D2LC01097F.

51. Brown, R.C., and Davis, T.P. (2002). Calcium Modulation of Adherens and Tight Junction Function. Stroke *33*, 1706–1711. https://doi.org/10.1161/01.STR.0000016405.06729.83.

52. Chung, R.S.K., Sum, P.T., Goldman, H., Field, M., and Silen, W. (1970). Effects of Chelation of Calcium on the Gastric Mucosal Barrier. Gastroenterology *59*, 200–207. https://doi.org/10.1016/S0016-5085(19)33761-8.

53. Muendoerfer, M., Schaefer, U.F., Koenig, P., Walk, J.S., Loos, P., Balbach, S., Eichinger, T., and Lehr, C.-M. (2010). Online monitoring of transepithelial electrical resistance (TEER) in an apparatus for combined dissolution and permeation testing. Int. J. Pharm. *392*, 134–140. https://doi.org/10.1016/j.ijpharm.2010.03.046.

54. Gitter, A.H., Wullstein, F., Fromm, M., and Schulzke, J.D. (2001). Epithelial barrier defects in ulcerative colitis: Characterization and quantification by electrophysiological imaging. Gastroenterology *121*, 1320–1328. https://doi.org/10.1053/gast.2001.29694.

55. Abdo, R., Jurjus, a., and Khoury a, N.N.; Jean-Marie Reimund (2004). Animal models of inflammatory bowel disease. J. Pharmacol. Toxicol. Methods *50*, 81–92. https://doi.org/10.1016/j.vascn.2003.12.002.

56. Adamkova, P., Hradicka, P., Kupcova Skalnikova, H., Cizkova, V., Vodicka, P., Farkasova Iannaccone, S., Kassayova, M., Gancarcikova, S., and Demeckova, V. (2022). Dextran Sulphate Sodium Acute Colitis Rat Model: A Suitable Tool for Advancing Our Understanding of Immune and Microbial Mechanisms in the Pathogenesis of Inflammatory Bowel Disease. Vet. Sci. *9*, 238. https://doi.org/10.3390/vetsci9050238.

57. Zheng, X., Xiong, T.-X., Zhang, K., Zhou, F.-C., Wang, H.-Y., Li, B., Dong, Y.-J., He, X., Li, L.-Z., Yu, Q.-X., et al. (2021). Benefit Effect of Dendrobium officinale Ultrafine Powder on DSS-Induced Ulcerative Colitis Rats by Improving Colon Mucosal Barrier. Evid. Based Complement. Alternat. Med. *2021*, 9658638. https://doi.org/10.1155/2021/9658638.

58. Sandle, G.I., and Rajendran, V.M. (2025). Ion transport and epithelial barrier dysfunction in experimental models of ulcerative colitis. Am. J. Physiol. Gastrointest. Liver Physiol. *328*, G811–G830. https://doi.org/10.1152/ajpgi.00204.2024.

59. González-Correa, C.A., Brown, B.H., Smallwood, R.H., Walker, D.C., and Bardhan, K.D. (2005). Electrical bioimpedance readings increase with higher pressure applied to the measuring probe. Physiol. Meas. *26*, S39–S47. https://doi.org/10.1088/0967-3334/26/2/004.

60. Lim, M.W., Stine, J.M., Ayansola, H., Holt, B.M., Beardslee, L.A., Kim, J., Chen, J., Jin, Y., and Ghodssi, R. (2025). In Vivo Bio-Impedance Sensing Capsule Study for Monitoring Mucosal Permeability in a DSS-Colitis Rat Model. In 2025 23rd International Conference on Solid-State Sensors, Actuators and Microsystems (Transducers), pp. 558–561. https://doi.org/10.1109/Transducers61432.2025.11109391.